Photodisintegration of Deuterium by 60- to 250-Mev X-Rays*

E. A. WHALIN,† BARBARA DWIGHT SCHRIEVER, AND A. O. HANSON
University of Illinois, Urbana, Illinois

(Received August 29, 1955)

A liquid deuterium target was irradiated with x-rays from the University of Illinois 300-Mev betatron. Exposures were made at maximum bremsstrahlung energies of 165 Mev, 280 Mev, and 300 Mev. The photoprotons produced were detected with Ilford *G*-5 nuclear emulsions. The distributions of protons as functions of energy were determined for laboratory angles of 30°, 45°, 75°, 120°, and 150°. In the energy region from 60 Mev to 250 Mev the angular distributions are relatively flat but have considerable fore and aft asymmetries. The total cross section, which was found not to vary greatly over this entire energy region, has a broad minimum of about 55 microbarns in the region of 150 Mev.

I. INTRODUCTION

EXPERIMENTAL information on high-energy photoprotons from deuterium is accumulating from nearly all laboratories which have high-energy x-ray sources. The earliest published results of Benedict and Woodward[1] and Gilbert and Rosengren[2] established the general features of the process and showed that there was an appreciable mesonic effect which increased the cross section for energies above 50 Mev.

Since that time other work has been done in an attempt to establish the cross section more quantitatively. Allen[3] has investigated the differential cross section in the energy region from 22 Mev to 65 Mev using nuclear plates. Keck, Littauer, O'Neill Perry, and Woodward[4] measured differential cross sections at a number of angles for 180 Mev and 260 Mev photons. Yamagata, Barton, Hanson, and Smith[5] investigated the differential cross section at laboratory angles of 45°, 75°, and 120° for photon energies between 140 Mev and 265 Mev. Extensive measurements at 5 angles using 340-Mev bremsstrahlung have been reported by Dixon.[6] Keck, Tollestrup, and Smythe[7] have data at 6 angles for photons between 100 Mev and 450 Mev. All these experiments and the work reported herein agree fairly well on the absolute magnitude of the cross section and the general features of the angular distribution in the region in which these overlap.

The results referred to have been obtained using scintillation counter range telescopes and give results which are statistically more accurate than the plate work described here. The plate data, however, give the only results in the energy region between 65 and 135 Mev. Results of the plate work leading to cross sections at higher energies will also be reported for completeness but the technique used had the disadvantage of giving poor energy resolution for high-energy protons.

Brief preliminary reports of the experiments described in this paper appeared earlier.[8,9]

II. EXPERIMENTAL PROCEDURES

A schematic diagram of the experimental setup is shown in Fig. 1. The x-rays from the 300-Mev betatron were collimated by a tapered hole in a lead block 33 cm thick, so that the beam diameter at the liquid deuterium target was 1.37 cm. A one-inch thick lead secondary collimator with a $\frac{1}{2}$-inch hole tapered 3 degrees was put in the end of the entrance arm of the target. A four-inch lead wall 6 inches high and 3 feet wide was built just behind the secondary collimator at a distance of 2.1 meters from the betatron x-ray source.

Protons from the reaction were incident on nuclear emulsions placed around the outside of the target. The nuclear plates were tipped at small angles to the equatorial plane to allow the observation of an appreciable length of track in the emulsions. Two separate exposures were made, one with a maximum energy of 165 Mev, the other with a maximum energy of 280 Mev. A later

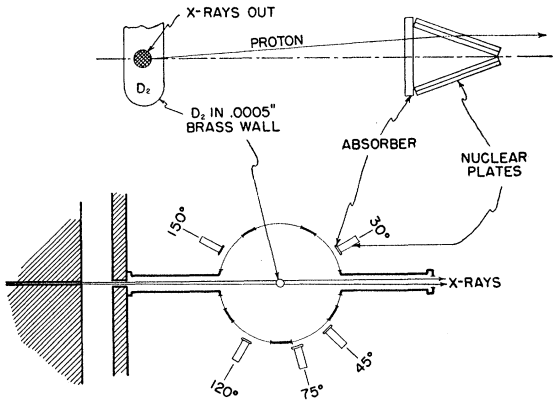

FIG. 1. Schematic diagram of apparatus.

* Work supported in part by the joint program of the Office of Naval Research and the U. S. Atomic Energy Commission.

† Present address, University of North Dakota, Grand Forks, North Dakota.

[1] T. S. Benedict and W. M. Woodward, Phys. Rev. **85**, 924 (1952).

[2] W. S. Gilbert and J W. Rosengren, Phys. Rev. **88**, 901 (1952).

[3] Lew Allen, Jr., Phys. Rev. **98**, 705 (1955).

[4] Keck, Littauer, O'Neill, Perry, and Woodward, Phys. Rev. **93**, 827 (1954).

[5] Yamagata, Barton, Hanson, and Smith, Phys. Rev. **95**, 575 (1954).

[6] Dwight R. Dixon, University of California Radiation Laboratory Report UCRL-2956, March 30, 1955 (unpublished).

[7] Keck, Tollestrup, and Smythe, Phys. Rev. **96**, 850 (1954).

[8] Schriever, Whalin, and Hanson, Phys. Rev. **94**, 763 (1954).

[9] E. A. Whalin, Jr., Phys. Rev. **95**, 1362 (1954).

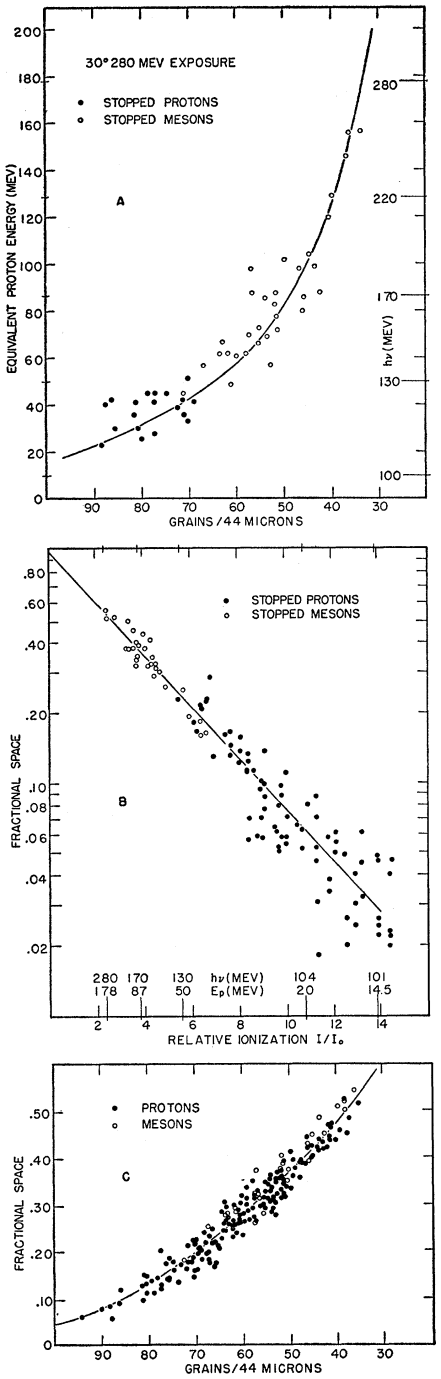

FIG. 2. Typical calibration curves. (*A*), Grain density as a function of proton energy determined from measurements on tracks of stopped mesons and protons. (*B*), Fractional space as a function of proton energy determined from measurements on stopped mesons and protons. (*C*), Correlation between fractional space and grain density for all tracks for which both quantities were measured.

check run was made at 300 Mev but the plates from this run were not completely analyzed.

The betatron electron target used was one of 0.020-inch platinum. The bremsstrahlung spectra used were the zero-angle thin-target spectra according to Schiff[10] as calculated by Leiss[11] with $C=191$ instead of 111. The integrated x-ray yields were measured using an 8-inch diameter flat copper ion chamber which has been calibrated calorimetrically by Kerst and Edwards.[12]

As shown in Fig. 1 the collimated x-ray beam passed through the middle of the liquid deuterium target, which was located at a distance of 2.6 meters from the x-ray source. This target had a diameter of 1.25 inches and a wall of 0.0005-inch brass foil. A detailed description of the liquid deuterium target has been published by Reitz and one of us (E.A.W.).[13]

The photoprotons which were produced in the liquid deuterium target passed through 0.005-inch copper foil windows in a radiation shield and through 0.017-inch aluminum windows in a vacuum jacket on their way to the detectors. The detectors were Ilford *G*-5 emulsions 600 microns thick on 1-inch by 3-inch glass plates. The plates were held in styrofoam cassettes with the long edges of the plates making angles of 30°, 45°, 75°, 120°, and 150° with the x-ray beam as shown in Fig. 1. The distance from the center of the liquid deuterium target to the front edge of the nuclear plates was 9 inches and the nominal included angle between the top and bottom plate in each cassette was 20 degrees.

For the 165-Mev exposures there were placed in front of the plates aluminum absorbers of such thickness that at every angle the protons produced by 60-Mev photons had an energy of about 8 Mev in the nuclear plates.

Runs at higher betatron energy were made with absorbers allowing the observation of protons originating from photons above 100 and above 160 Mev. The exposure conditions are given in Table I. The plates at 30° in the 165-Mev run were removed about midway in the exposure to prevent them from getting too dark. Comparable exposures were made with the target empty. The plates were developed using a dry development technique.[14]

III. ACCUMULATION OF DATA

The plates were scanned using Leitz Ortholux binocular microscopes. The area scanned at different angles was varied so that observations were made on about 500 protons on each data plate. Less area was read on the background plates and the number of protons recorded were multiplied by the correct ratio to obtain the background at each angle.

The coordinates of all tracks starting in the surface of the emulsion in the areas scanned were recorded. Next the azimuth angles of the tacks as they entered the plates were measured. The azimuth angle was measured in the plane of the emulsion relative to the

[10] L. I. Schiff, Phys. Rev. **83**, 252 (1951).
[11] J. E. Leiss (privately circulated tables).
[12] D. W. Kerst and P. D. Edwards, Rev. Sci. Instr. **24**, 490 (1953).
[13] E. A. Whalin, Jr., and R. A. Reitz, Rev. Sci. Instr. **26**, 59 (1955).
[14] A. Beiser, Revs. Modern Phys. **24**, 273 (1952).

long 3-inch dimension of the plate i.e., an azimuth angle $\sim 0°$ indicated the track came from the direction of the liquid deuterium target. No further measurements were made on tracks whose azimuth angle exceeded $\pm 20°$.

If a track had an azimuth angle less than $\pm 20°$ the following measurements were also made:

(1) The final coordinates of the track in the plate.
(2) The final azimuth angle of the track.
(3) The depth in the emulsion at which the track stopped. If the track left the bottom of the emulsion this was noted but the thickness of the emulsion was not measured.
(4) The range projected into the plane of the plate if the track stopped in the emulsion. This measurement was made with a calibrated reticule in one of the oculars.
(5) A space measurement and/or grain count if the track passed through the emulsion without stopping.
(6) Multiple scattering measurements on high-energy tracks in the 280-Mev exposure to distinguish between mesons and protons of similar ionization.

These measurements were made on a segment of the track 450 microns long and started at a point on the track about 20 microns under the emulsion surface. In the final treatment of the data only tracks with initial azimuth angles of less than ± 15 degrees were retained. This limit was selected because between 15 and 20 degrees there were about as many tracks on the background plates as on the data plates. No tracks were retained for further analysis whose projected length from the surface to the bottom of the emulsion was less than 1.4 mm, i.e., whose dip angle was greater than 25 degrees. The dip angle of a line from the center of the liquid deuterium target to an emulsion surface was 13 degrees. No tracks were retained whose ranges were less than 300 microns. This range corresponds to a proton energy of 7 Mev. This lower energy limit was selected to avoid large scattering losses.

The energies of the protons which stopped in the plates were determined from their ranges in the emulsion by using the range-energy relations of Wilkins.[15] The ranges projected into the planes of the plates were corrected for the dip of the tracks. The ranges were also adjusted for the effect of humidity on the emulsion density by using Wilkin's data.

The energies of the protons which passed through the emulsion were determined by the use of one of two methods, by counting the number of silver grains in a length of track or by measuring the amount of open space between silver grains in a length of track. The former method was used for high-energy protons leaving sparse tracks and the latter method for low-energy protons leaving dense tracks. In the 280-Mev exposure both space and grain density were measured for protons of 90 to 130 Mev. The grain counts and space measurements were converted into energies by comparing them with grain counts and space measurements made on π-meson tracks which ended in the emulsion. A π meson and a proton producing the same initial ionization along their paths in the emulsion have ranges proportional to their respective masses. It proved possible therefore to find π-meson tracks ending in the emulsion whose initial ionizations corresponded to the entire range of proton energies produced in the experiment.

[15] J. J. Wilkins, Atomic Energy Research Establishment, Harwell Report, *G/R* 664, 1951 (unpublished).

TABLE I. Exposure conditions.

	Thickness of absorbers in front of plates at the given angle in inches of aluminum					Length of run Minutes	X-ray flux thru target Ergs
	30°	45°	75°	120°	150°		
Equivalent absorption in D_2 target and walls	0.084	0.079	0.076	0.078	0.084	...	...
165 Mev 60-Mev absorbers	0.120	0.108	0.078	0.021	0.0	140	3.33×10^8
280 Mev 100-Mev absorbers	0.490	0.447	0.327	0.170	0.114	45	3.47×10^8
300 Mev 160-Mev absorbers	...	1.230	0.866	...	0.325	90	5.82×10^8

Figure 2 show typical calibration curves for the grain counting and space measuring methods of determining energy as well as the correlation between the two methods. Assuming the deviations from the curves drawn were fitted by an error function, the standard deviations in proton energy by grain counting and by space measurement was about 15%.

There were, of course, some mesons produced in the deuterium target which had to be distinguished from the protons which were the concern of these experiments. In the 165-Mev plates, the few mesons present were of fairly low energy and readily identified by inspection. To distinguish between high-energy proton and meson tracks on the plates exposed at 280 and 300 Mev, multiple-scattering measurements were made using the Fowler[16] method.

IV. TREATMENT OF DATA

The proton energies as determined by space and grain density measurements were transformed into their initial values in the deuterium target by using Aaron's[17] range-energy curves for the energy loss in the target and in the different absorbers. The corresponding photon energies were obtained from the kinematical relations tabulated by Malmberg and Koester.[18]

The proton spectra were divided into wide bins for the purpose of computing cross sections. This was

[16] P. H. Fowler, Phil. Mag. **41**, 169 (1950).
[17] W. A. Aaron, University of California Radiation Laboratory Report UCRL-1325, 1951 (unpublished).
[18] J. H. Malmberg and L. J. Koester, Jr., *Tables of Nuclear Reaction Kinematics at Relativistic Energies* (Physics Department, University of Illinois, 1953).

TABLE II. Experimental cross sections for the photodisintegration of deuterium. The starred symbols refer to the center-of-mass system. A correction for nuclear attenuation based on $\sigma_{Al}=1.1$ barns has been applied to all cross sections. The value for $\theta=30°$, $h\nu=114$ is large because of the contribution of π^0 protons produced by photons above 270 Mev.

θ_{lab} Deg	$h\nu_{lab}$ Mev	$d\sigma/d\Omega_{lab}$ μb/sterad	$d\sigma^*/d\Omega$ μb/sterad	θ^* Deg	Betatron energy Mev	Minimum energy Mev
	65	9.5±0.6	7.6±0.5	33.8		
	80	8.8±0.6	7.0±0.5	34.2	165	60
	105	7.7±0.5	5.9±0.4	34.8		
	140	7.0±0.5	5.1±0.4	35.6		
30						
	114	(15.5±0.8)	(11.6±0.6)	35.1		
	149	6.9±0.5	5.0±0.4	35.8	280	100
	194	9.2±0.7	6.4±0.5	36.7		
	248	9.0±0.7	6.0±0.5	37.5		
	65	13.3±0.9	11.2±0.8	50.4		
	80	10.0±0.8	8.2±0.7	51.0	165	60
	105	8.2±0.6	6.6±0.5	51.8		
	140	7.0±0.6	5.4±0.5	52.9		
45						
	114	10.3±0.6	8.2±0.5	52.3		
	149	7.4±0.5	5.7±0.4	53.3	280	100
	194	10.5±0.7	7.9±0.5	54.4		
	248	6.0±0.6	4.3±0.4	55.7		
	220	7.6±0.8	6.0±0.6	55.0	300	160
	65	11.4±0.7	10.7±0.7	82.4		
	80	7.4±0.5	7.0±0.5	83.2	165	60
	105	7.9±0.5	7.3±0.5	84.3		
	140	5.1±0.4	4.7±0.4	85.8		
75						
	114	7.0±0.5	6.5±0.4	84.8		
	149	5.3±0.4	4.9±0.4	86.2	280	100
	194	7.8±0.6	7.2±0.5	87.8		
	248	5.4±0.5	4.9±0.5	89.4		
	220	6.3±0.6	5.8±0.5	88.6	300	160
	65	6.5±0.4	7.5±0.4	126.6		
	80	3.4±0.3	4.0±0.3	127.3	165	60
	105	2.9±0.2	3.4±0.2	128.3		
	140	3.3±0.2	4.2±0.3	129.5		
120						
	114	3.5±0.2	4.3±0.3	128.6		
	149	2.6±0.2	3.2±0.3	129.8	280	100
	194	4.2±0.3	5.4±0.4	131.3		
	248	3.5±0.3	4.7±0.4	132.6		
	65	3.3±0.2	4.2±0.3	153.8		
	80	3.1±0.2	4.1±0.3	154.2	165	60
	105	2.6±0.2	3.6±0.2	154.8		
	140	1.2±0.1	1.8±0.2	155.5		
150						
	114	2.7±0.3	3.7±0.4	155.0		
	149	1.6±0.3	2.3±0.4	155.7	280	100
	194	2.1±0.3	3.4±0.5	156.5		
	248	2.1±0.3	3.6±0.6	157.2		
	220	2.2±0.3	3.5±0.4	156.8	300	160

possible because the cross sections vary rather slowly in the energy region covered by the experiment and it was desirable because of the small number of protons measured and the uncertainty in their energies. An exception to this was the first bin of the 165-Mev run. This bin was selected to consist only of stopped protons because the larger cross sections at this lower energy permitted taking a narrow energy bin that had good statistics. It also permitted getting a point for direct comparison with the work of Allen.[3] The other energy bins varied in width from 20 to 60 Mev. The width was varied so that approximately equal numbers of protons were included in each bin. The highest energy bins in each exposure were also made the widest for the purpose of minimizing the effect of the uncertainty in the maximum photon energy.

The average differential cross section for an energy bin is defined by the formula:

$$d\sigma_E/d\Omega=N_p/N_\gamma N_D\Delta\Omega,$$

where $d\sigma_E/d\Omega$ is the average differential cross section for a photon energy bin of average energy E, in cm²/steradian, N_p is the number of protons counted at a given angle produced by photons in the energy bin, N_γ is the number of photons in the energy bin, N_D is the number of deuterium atoms per cm² presented by the liquid deuterium target, and $\Delta\Omega$ is the solid angle presented to the source by the plate surface scanned.

Of the four factors which enter into the calculation of a cross section, N_D is known with an uncertainty of less than 1% and $\Delta\Omega$ with an uncertainty of about 3%. These are small compared to other errors. The number of photons in all bins have a possible error of about 5% due to the uncertainty in the measurement of the total energy in the photon beam and to the lack of precision in our knowledge of the photon spectrum. There are additional errors in the values of N_γ for the highest energy bins since N_γ is very sensitive to the precise values used for the effective maximum energy of the bremsstrahlung spectra. This error depends on the size of the top bin and is estimated to be about 15% for both the 165 Mev and the 280-Mev runs.

The number of protons, N_p, has a statistical error of 10% or less in almost all cases. The error due to scanning efficiency is negligible since extensive checking disclosed virtually no missed tracks. The uncertainties in the proton energies however, introduce errors in the number of protons assigned to a photon energy bin which are usually larger than the statistical uncertainty based on the number of protons in the bin.

Although there were a large number of tracks left by mesons passing through the plate, only a few had grain densities high enough to be confusable with protons and most of these were clearly separated by multiple scattering measurements. There may be a few confusable mesons in the highest energy bin for forward angles in the high-energy exposures. Mesons should cause negligible errors for all other bins.

Losses due to multiple scattering of the protons were assumed to be negligible because of the small calculated rms scattering angle (4 degrees or less for the proton energies used in the experiment) and because of the fact that most of the scattering material was in poor geometry with respect to the plates.

The proton spectra were corrected for nuclear absorption and scattering loss, however, by converting

the material the protons passed through in reaching the plates from the target to equivalent amounts of aluminum and assuming the total nuclear cross section to be twice the geometrical, i.e., 1.1 barns. The losses calculated in this way varied from 1.2% to 18%.

The background protons were obtained from a plate exposed under the same conditions as the data plate except that the brass deuterium container was empty. The background measured in this way varied from 5% to 13% on the different plates.

The absolute uncertainties in the cross sections range from about 10% in the most favorable cases to about 25% in the least favorable.

The results of the cross-section calculations are given in Table II. These are arranged according to the angle of the plate in the laboratory system. In addition to the average photon energy in each bin the table also presents the center-of-mass angle and the cross section in the center-of-mass system. The errors listed are only the rms statistical errors based on the number of protons observed. The magnitude and angular distribution of the cross section for the 194- and 248-Mev bins show greater differences than that obtained in the counter experiments. This discrepancy has been of some concern since it could arise from a systematic error in determining the proton energies in the plates. Checks on stopped mesons and protons however, disclosed no obvious systematic errors. The average of these two bins, however, give results in good agreement with the wide bin in the 300-Mev run as well as with counter work.

V. EMPIRICAL SYNTHESIS OF THE DATA

The experimental data from Table II are shown as a function of energy and angle in Fig. 3. The solid lines in this figure are of the form $d\sigma^*/d\Omega=(A+B\sin^2\theta^*)(1+2\beta\cos\theta^*)$. This form was suggested by the retardation effect and was useful in discussing the lower energy results. The values of A, B, and β were obtained empirically from the cross sections given with the additional requirements that the cross section at any angle is a smooth function of energy. These are given in Table III. A least squares determination of A and B from the unsmoothed data for each energy bin gave values in general agreement with the smoothed values in the table and indicated variations in A and B of about 1 μb/sterad. The total cross section is relatively more accurate than either A or B since it is not very sensitive to the detailed fit of the differential cross-section curves, and has a statistical error of about 10%. It is also subject to systematic errors of about 5% as mentioned earlier. The table also gives the isotropic and the $\sin^2\theta^*$ parts of the cross section as well as the total cross section expressible as $4\pi A+8\pi B/3$. The total cross section and the two components are shown as a function of energy in Fig. 4. Here one can see that the isotropic component of the cross section varies only slightly from 22 to 250 Mev while the $\sin^2\theta^*$ component decreases markedly in this interval.

The retardation parameter (β) increases up to a maximum near the meson photothreshold and then varies more slowly. It is doubtful whether the asymmetry expressed in terms of this parameter can be interpreted as a retardation effect at the higher energies where meson effects are important. Tollestrup, Keck, and Smythe as well as Dixon use the expression

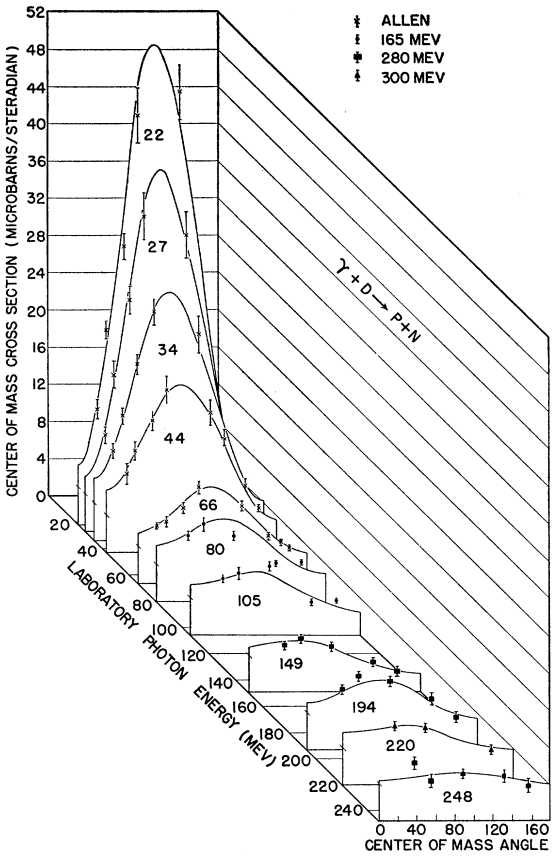

FIG. 3. Differential cross sections in the center-of-mass system as a function of the center-of-mass angle for various laboratory photon energies. The data of Allen at lower energies are also shown. The curves are of the form $(A+B\sin^2\theta^*)(1+2\beta\cos\theta^*)$ using the coefficients given in Table III.

TABLE III. Values of A, B, and β from the relation $(A+B\sin^2\theta^*)\times(1+2\beta\cos\theta^*)$ representing the cross section. The isotropic part, the $\sin^2\theta^*$ part, and the total cross sections are given in the last three columns.

$h\nu$ Mev	2β	A μb/sterad	B μb/sterad	$4\pi A$ μb	$8\pi B/3$ μb	σ_{total} μb
65	0.25	5.0	5.7	62	47	109
80	0.35	4.5	3.9	56	32	88
105	0.38	3.9	2.2	49	18	67
140	0.40	3.4	1.3	43	11	54
114	0.40	5.3	0.9	67	7	74
149	0.44	3.5	1.2	44	10	54
194	0.22	4.2	2.9	53	24	77
248	0.10	4.2	0.9	53	11	64
220	0.22	4.5	1.3	57	11	68

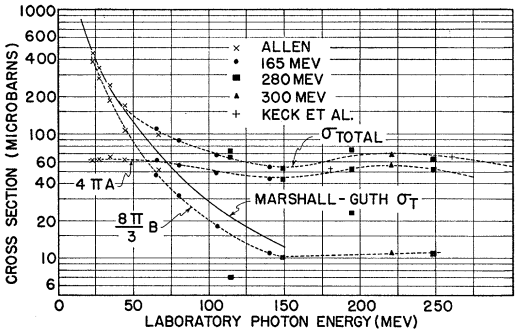

FIG. 4. The total cross section as given by $4\pi A+8\pi B/3$. The isotropic component $4\pi A$ and the $\sin^2\theta^*$ component $8\pi B/3$ are shown as a function of energy. The solid line is the total cross section as calculated by Marshall and Guth.

$A'+B'\cos\theta^*+C'\cos^2\theta^*$ to represent their results. This expression is identical to the one used here if one neglects the $\sin^2\theta^*\cos\theta^*$ term except that $A'=A+B$, $B'=2A\beta$ and $C'=-B$.

VI. DISCUSSION

Up to 150 Mev the $\sin^2\theta^*$ part of the total cross section may be adequately explained by the phenomenological theories of Schiff[19] and Marshall and Guth[20] which omit any explicitly mesonic effects. The agreement of the $\sin^2\theta^*$ part of the total cross section, $8\pi B/3$, with the total cross section calculated by Marshall and Guth can be seen from the curves of Fig. 4. Marshall and Guth, and Schiff restricted their calculations to interactions involving only central potentials. An appreciable isotropic component in the angular distribution can arise from noncentral forces as was shown by Rarita and Schwinger[21] and by Hu and Massey.[22] Austern[23] has extended these considerations up to energies of about 100 Mev and showed that an appreciable isotropic component can arise from any strongly singular noncentral force. In particular he found an isotropic component of the correct order of magnitude from the singular L-S force used by Case and Pais[24] in the treatment of nuclear scattering. Qualitatively this interaction can be seen to favor transitions to the $^3P_0$ state over those to the $^3P_1$ and $^3P_2$ states and would therefore contribute to an isotropic distribution. Austern stated, however, that the magnitude as well as the energy dependence of this isotropic component is largely due to the strongly singular nature of the interaction.

Yamaguchi and Yamaguchi[25] have considered the two-nucleon problem using a nonlocal but separable interaction. They felt the separable potentials they used could be used in the calculation of the photodisintegration of deuterium cross sections for an energy up to about 50 Mev. They performed these calculations for the electric dipole and also for the magnetic dipole interaction, neglecting in the latter case the interaction magnetic moment. The magnetic dipole cross section is very small, but there is an increasing isotropic component above 10 Mev arising from an electric dipole transition from the ^3D part of the ground-state wave function to the final ^3P states. It turns out, however, that the resulting isotropic part is too small to explain the observed results even if the D state is as large as 8%.

Another possible explanation of the isotropic part of the total cross section is of interest. Perhaps instead of arising from an interference effect, the isotropic part of the total cross section is actually due to a process which produces a nonintefering isotropic term. It is strongly suspected that this isotropic component arises from mesonic processes, since mesonic effects should become important in this energy range. The fact that low-energy photomesons are also emitted isotropically suggests a connection between photodisintegration and photomeson processes.

In order to isolate a possible mesonic contribution from the experimental observations, it was assumed that the Marshall and Guth[20] theory accounts for the cross section derivable from a simple nuclear force. The Marshall and Guth total cross section was then subtracted from the observed total cross section. This difference which may be tentatively attributed to specific mesonic interactions, is shown in Fig. 5. Since mesonic effects are involved in some approximation in order to get agreement with the experiments at low energies, the fact that the difference appears to vanish at 40 Mev is perhaps not significant. This effect can be interpreted as a slowing rising contribution to the cross section which varies approximately with the momentum of the outgoing protons. This contribution could be described then as due to a constant matrix element which shows no change as the energy increases above the threshold for real meson production. This result implies that the photoproton production does not compete with the photopion production above the threshold.

This can be understood in terms of an argument of Wilson[26] that when a virtual or real absorption of a photon by the meson field takes place in a small volume, having a radius less than the pion Compton wavelength also occupied by more than one nucleon the coupling to the nucleon field is so strong that nucleons and pions are emitted with probabilities governed only by their statistical weights and momenta. Since for a given excitation energy the momentum available to the nucleons is much larger than that available to the pions,

[19] L. I. Schiff, Phys. Rev. **78**, 733 (1950).
[20] J. F. Marshall and E. Guth, Phys. Rev. **78**, 738 (1950).
[21] W. Rarita and J. S. Schwinger, Phys. Rev. **59**, 556 (1941).
[22] T. Hu and H. S. W. Massey, Proc. Roy. Soc. (London) **A196**, 135 (1949).
[23] N. Austern, Phys. Rev. **85**, 283 (1952); also private communication.
[24] K. M. Case and A. Pais, Phys. Rev. **80**, 203 (1950).
[25] Y. Yamaguchi and Y. Yamaguchi, Phys. Rev. **95**, 1635 (1954); Phys. Rev. **98**, 69 (1955).
[26] R. R. Wilson, Phys. Rev. **86**, 125 (1952).

the result in most cases will be nucleon emission. The fraction of the time the neutron and proton in the deuteron can be considered as less than $\hbar/\mu c$ apart can be obtained from the ground state wave function. Using the wave function as given by Schiff[19] for a Hulthén potential, one obtains 3.6 for the ratio of photomeson cross section to photoproton cross section. This is in qualitative agreement with the observed ratio of about 7 at 250 Mev.[27,28] This model also assumes that the interaction of the photons with the meson field is independent of the surrounding nucleons. This agrees with the fact that the sum of the cross sections for the production of pions and of protons from deuterium is very nearly twice the cross section for the production of pions from hydrogen. In complex nuclei the cross section for pion production goes up only as $A^{\frac{1}{3}}$, which indicates that pions are produced from surface nucleons. The star production which is predominant also above the meson threshold is then an indication of the close coupling between pions and nucleons.

The data from the present experiment indicate roughly that the pion contribution to the photodisintegration cross section is not much affected by the threshold for real pion production. Further results on the yield of protons from other nuclei below and above the meson threshold may be helpful in clarifying this point. A study of photon scattering from deuterium above and below the meson threshold may also be helpful in determining if the photoproton cross section arises mainly from an intermediate meson state.

A specific meson reabsorption model which contributes to an isotropic angular distribution is suggested by the electric dipole absorption which is responsible for low energy photomeson production. This transition ends up with the nucleon spin flipped and the meson, which has odd parity in an S state.[29] In the case of the deuteron an elementary attempt can be made to use the same interaction with one of the nucleons to reach an intermediate state which contains a pion in an S state and the nucleons in antiparallel spin states. The total angular momentum of this state would be zero. After reaching this state reabsorption of the meson would put the nucleons in an odd parity state with $J=0$, or a $^3P_0$ state. This state would be one of the ^3P states considered in the theories using noncentral forces as interfering with each other to give rise to the growing isotropic component in the lower energy region. If, however, this transition arises from a separable spin interaction as distinguished from an orderinary potential interaction, the additional component arising from this virtual meson effect may be added to the cross section due to charge transitions without interference. Although such an interaction could explain the observed results, it seems to require a stronger coupling between nucleons and pions in S states than is indicated by scattering experiments.

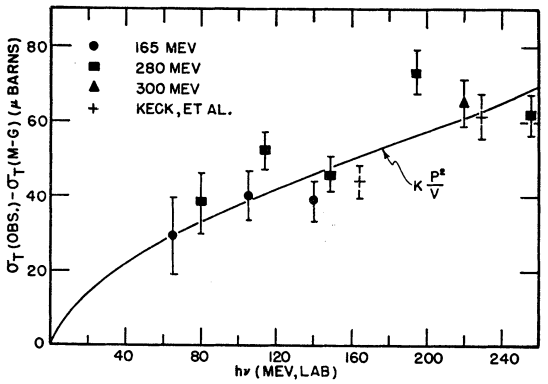

FIG. 5. Difference between the experimental total cross section and the total cross section calculated by Marshall and Guth. The solid line represents a function p^2/v which is proportional to the energy density of final states, where p is the momentum and v is the velocity of the outgoing protons in the center-of-mass system.

The observed features of the mesonic part of the photoproton cross section can also be explained in terms of a magnetic dipole transition which would give rise to an isotropic noninterfering contribution. Nagahara and Fujimura[30,31] and Bruno and Depken[32] have made calculations of the exchange magnetic moment contribution using a phenomenological operator and a singular radial dependence. They obtained in this way a contribution to the cross section of about the right magnitude. There is, however, no detailed confirmation of a large exchange magnetic moment from other experiments.

At energies around 300 Mev corresponding to the $I=\frac{3}{2}$, $J=\frac{3}{2}$ resonance in the pion nucleon system one expects an increase in photoprotons as a consequence of the increased photon absorption. A model in which the reaction proceeds through this resonance has been discussed by Austern.[33] He finds that this model leads to an angular distribution of $2+3\sin^2\theta^*$ and a magnitude given approximately by 9/4 of the cross section for π^0 photoproduction times the ratio of π^+ absorption in deuterium to the scattering of π^+ mesons in hydrogen. This relation between photoproton and photopion cross sections is apparent in the experimental results at higher energies where both cross sections fall off toward 450 Mev in a similar way. It accounts for approximately one-half the maximum in the experimental cross section.

It is of some interest to compare the observed integrated cross section with that obtained from various sum rules. The present results give an integrated cross section up to meson threshold of 0.38-Mev barns. This corresponds to a 30% increase over the Thomas-

[27] Jenkins, Luckey, Palfrey, and Wilson, Phys. Rev. 95, 179 (1954).
[28] G. Cocconi and A. Silverman, Phys. Rev. 88, 1230 (1952).
[29] G. F. Chew, Phys. Rev. 95, 1669 (1954).
[30] Y. Nagahara and J. Fujimura, Progr. Theoret. Phys. (Japan) 8, 49 (1952).
[31] J. Fujimura, Progr. Theoret. Phys. (Japan) 9, 132 (1953).
[32] B. Bruno and S. Depken, Arkiv. Fysik. 6, 177 (1953).
[33] N. Austern, Phys. Rev. 87, 208 (1952), and private communication.

Reich-Kuhn value for electric dipole transitions for ordinary forces, and can be attributed to meson effects. A detailed discussion of the integrated cross section in terms of various sum rules is given by Levinger.[34]

ACKNOWLEDGMENTS

It is a pleasure to acknowledge the assistance received from G. Bernardini, E. L. Goldwasser and R. A. Reitz during the exposure and development of the plates and the helpful discussion with them since. The authors are indebted to Nella Bernardini, Elizabeth Hanson, Bernice Pope, Joan Terwilliger, J. M. Gaston, J. Impeduglia, D. J. Knecht, J. Spiegelman, and E. Upitis for their assistance in scanning the nuclear plates. They appreciate discussions concerning theoretical work with G. F. Chew, Yoshio Yamaguchi, I. Hodes, and N. Austern and communications regarding experimental work from J. Keck and D. Dixon.

[34] J. S. Levinger, Phys. Rev. **97**, 970 (1955).

PHYSICAL REVIEW VOLUME 101, NUMBER 1 JANUARY 1, 1956

Total Cross Sections for Scattering and Absorption of Pions by Nuclei*

R. M. STERNHEIMER
Brookhaven National Laboratory, Upton, New York
(Received September 7, 1955)

The causality conditions of Goldberger for the pion-nucleon scattering have been used to calculate the parameter k_1 of the optical model for scattering of pions from nuclei. These values of k_1 together with values of the absorption coefficient K in nuclear matter were used to obtain the total absorption and diffraction cross sections of pions for carbon, copper, and lead in the range 0–2.5 Bev.

IT has recently been shown by Karplus and Ruderman[1] and by Goldberger[2] that the real part of the forward scattering amplitude for the pion-nucleon scattering can be obtained from a knowledge of the π^+-p and π^--p total cross sections at all energies. This relation has been called the causality condition, and has been used by Anderson, Davidon, and Kruse[3] to calculate the real part of the forward scattering amplitude for the π^+-p and π^--p scattering for energies up to 240 Mev, using the measured total cross sections in the range 0–1.9 Bev. A knowledge of the real part of the forward scattering amplitude would enable one to calculate the total cross section for diffraction scattering of pions by nuclei, if one makes use of the optical model[4] of the nucleus.[5] In the present work, the parameters k_1 and K of the optical model are determined as a function of energy in the range 0–2.5 Bev, and the total pion cross sections are calculated for C, Cu, and Pb. It is assumed that k_1 and K have constant values in the interior of the nucleus and drop sharply to zero at the nuclear radius R which was taken as $1.4\times10^{-13}\,A^{\frac{1}{3}}$ cm.

The parameter k_1 which measures the change of wave number as the pion enters the nucleus is given by

$$k_1=2\pi\rho[ZD_{\pm}(k)+(A-Z)D_{\mp}(k)]/(kA), \quad (1)$$

where the upper and lower signs pertain to π^+ and π^- scattering, respectively; ρ=density of nucleons; k=wave number; $D_+(k)$ and $D_-(k)$ are the real parts of the forward amplitude for π^+-p and π^--p scattering, respectively. Goldberger, Miyazawa, and Oehme[2] have obtained the following equations for $D_+(k)$ and $D_-(k)$:[6]

$$D_+(k)=\frac{1}{2}\left(1+\frac{\omega}{\mu}\right)D_+(0)+\frac{1}{2}\left(1-\frac{\omega}{\mu}\right)D_-(0)+\frac{k^2}{4\pi^2}\int_\mu^\infty\frac{d\omega'}{k'}\left[\frac{\sigma_+(\omega')}{\omega'-\omega}+\frac{\sigma_-(\omega')}{\omega'+\omega}\right]+\frac{2f^2}{\mu^2}\frac{k^2}{\omega-(\mu^2/2M)}, \quad (2)$$

$$D_-(k)=\frac{1}{2}\left(1+\frac{\omega}{\mu}\right)D_-(0)+\frac{1}{2}\left(1-\frac{\omega}{\mu}\right)D_+(0)+\frac{k^2}{4\pi^2}\int_\mu^\infty\frac{d\omega'}{k'}\left[\frac{\sigma_-(\omega')}{\omega'-\omega}+\frac{\sigma_+(\omega')}{\omega'+\omega}\right]-\frac{2f^2}{\mu^2}\frac{k^2}{\omega+(\mu^2/2M)}, \quad (3)$$

* Work performed under the auspices of the U. S. Atomic Energy Commission.

[1] R. Karplus and M. A. Ruderman, Phys. Rev. **98**, 771 (1955).

[2] M. L. Goldberger, Phys. Rev. **99**, 979 (1955); Goldberger, Miyazawa, and Oehme, Phys. Rev. **99**, 986 (1955).

[3] Anderson, Davidon, and Kruse, Phys. Rev. **100**, 339 (1955). I would like to thank Professor Anderson for sending me a copy of this paper in advance of publication.

[4] Fernbach, Serber, and Taylor, Phys. Rev. **75**, 1352 (1949); H. A. Bethe and R. R. Wilson, Phys. Rev. **83**, 690 (1951).

[5] I would like to thank Dr. Piccioni for calling my attention to this point.

[6] The units are such that $\hbar=c=1$.